COBEM 2023 27TH INTERNATIONAL CONGRESS OF MECHANICAL ENGENEERING

ABCM Brazilian Society of Mechanical Sciences and Engineering
27th ABCM International Congress of Mechanical Engineering
December 04-08, 2023, Florianópolis-SC, Brazil

COB-2023-2149
POWDER METALLURGICAL MANUFACTURING OF GRAPHENE REINFORCED TITANIUM COMPOSITES

Fernanda Signor
Gabriela Emanuelle Valeriano Soares de Souza
Sérgio Noal Alves
Maurício Covaleski Zubaran
Paulo Henrique Mareze
Natália de Freitas Daudt
Federal University of Santa Maria, Av. Roraima nº 1000 Cidade Universitária Bairro - Camobi, Santa Maria - RS, 97105-900
fernanda.signor@acad.ufsm.br gabriela.soares@acad.ufsm.br sergio.noal@acad.ufsm.br mauricio.zubaran@acad.ufsm.br
paulo.mareze@ufsm.br natalia.daudt@ufsm.br

Abstract. *Titanium shows a combination of mechanical strength, corrosion resistance and biocompatibility, which makes it a structural material for aerospace and biomedical applications. However, titanium has lower stiffness when compared to other aerospace materials. An alternative to increase titanium stiffness is the use of metal matrix composite (MMCs) reinforced with nanoparticles. Graphene has been reported as a promising reinforcement for MMC due its combination of stiffness, strength, low density, thermal and antimicrobial properties. Therefore, graphene reinforced titanium is attractive for both biomedical and aerospace industries. In this work, manufacturing of graphene-reinforced titanium composites using powder metallurgy routes was investigated. For that, Ti parts with graphene addition varying from 0.2 to 0.5 wt were produced by warm compaction of MIM feedstocks and cold compaction of 3D extrusion pastes. The results obtained so far demonstrate that by adjusting the graphene amount samples with higher elastic modulus can be produced.*

Keywords: *Titanium-Graphene, Metal Matrix Composite, Powder Metallurgy, Mechanical Test, Vibroacoustic Test.*

1. INTRODUCTION

Powder Metallurgical (PM) process has emerged as a highly advantageous technique, combining cost-effectiveness, efficiency, and the possibility to manufacture an array of complex parts with precision. PM has increased its importance due to Additive Manufacturing (AM), mainly by the new sinter-based 3D printing techniques. The convergence of PM, and AM has opened up new possibilities in the production of complex parts with enhanced efficiency. Additive manufacturing techniques, such as 3D printing, enable the layer-by-layer construction of components using powder. In this context, PM stands out as an ideal process due to its ability to produce finely controlled metal powders, ensuring the requisite quality, and characteristics for successful additive manufacturing applications Gialanella and Malandruccolo (2020).

According to Hayat *et al.* (2018), in recent years, Metal Inject Molding (MIM) has gained significant attention as a cost-effective production process for various industries. Research conducted by Baril *et al.* (2008) highlights the advantages of MIM in terms of complex geometries, high precision and material utilization. Studies demonstrate the successful application of MIM in the production of small-sized, intricate components with excellent mechanical properties in various industries, including biomedical, military, electronics, automotive, aerospace, and chemicals as emphasized by Dehghan-Manshadi *et al.* (2017). MIM is especially suitable for large scale production of small parts with complex shaped. In the other hand AM technologies based on sintering can be attractive for small scale production of complex shaped parts in different sizes.

According to Nurhudan *et al.* (2021) 3D extrusion of metal pastes has emerged as a promising technology in additive manufacturing of complex metal components. Its advantages encompass various aspects, such as the ability to produce parts with intricate geometries and fine details, enabling the fabrication of customized and high-performance structures. Moreover, the use of metal pastes provides flexibility in working with diverse materials, including specialized metal alloys. As a result, the 3D extrusion of metal pastes has been increasingly applied in various sectors, including aerospace, automotive, healthcare, and engineering as emphasized by Rane and Strano (2019).

Powder metallurgy, known for its advantageous production characteristics such as dimensional accuracy, control over porosity, and waste reduction, has garnered attention in the study of composite materials (Saxena *et al.*, 2023). Composite materials founded extensive use in various industries for the production of lightweight components and structures. These materials can be classified based on the type of matrix or reinforcement used. With respect to the matrix, options include

polymeric, ceramic, and metallic, while the reinforcement can be in the form of fibers, particles, or sheets. Metal Matrix Composites (MMCs) have gained considerable prominence, particularly with the utilization of graphene as a reinforcement material (Gorbatikh *et al.*, 2016).

Szunerits *et al.* (2015) studied graphene forms, in addition to its flat form, graphene can be rolled into nanotubes or appear in alternative allotropic forms such as graphite or fullerene. Furthermore, graphene can exist in an oxidized form. The process of oxidizing graphite using strong oxidants results in the formation of graphene oxide (GO). By employing reducing agents, graphene oxide can be converted into reduced graphene oxide (rGO).

Hu *et al.* (2018) investigated the fabrication of graphene-titanium composites using laser sintering and PVA bonding with graphene-titanium coating. They find a well-integrated microstructure and a uniform distribution of graphene with the matrix (Ti). Graphene as a reinforcement material improved mechanical properties compared to pure titanium. Cao *et al.* (2017) fabricated a Ti6Al4V matrix composite reinforced with graphene homogeneously using powder metallurgy techniques. The study observed the formation of TiC particles, which effectively reinforced the interface Ti-Gr.

This article focuses on analyzing the feasibility of producing titanium-graphene composites from MIM and 3D extrusion feedstocks. The main objective of this study is to evaluate the practicality and viability of utilizing those formulations for the fabrication of composite materials incorporating titanium and graphene. The warm compaction method was chosen due to its similarity with MIM and the possibility to process a small amount of materials. The cold compaction of 3D extrusion feedstock was chosen to evaluate feedstock materials for 3D extrusion, which is an emerging technology. Both methods offer valuable insights for enhancing understanding of the process and its potential applications in additive manufacturing.

2. MATERIALS AND METHODS

2.1 Materials

Experiments were carried out by using titanium and graphene powders, both supplied by Alfa Aesar. The commercially pure (99.5%) grade 2 titanium powder, with irregular shape and particle size smaller than 45 μ, was used as matrix. The graphene powder, consists of aggregates of submicroparticles graphene nanoplatelets (GNPs), with superficial area < 500 m^2/g, which are individual nanoparticles composed of small overlapping graphene sheets was used as a reinforcement material. The preparation of feedstocks used in this study involved two different processes, one for the MIM feedstock and another for 3D extrusion feedstock.

The binder system of MIM feedstocks composed of 5wt% stearic acid (SA), 70wt% paraffin (PW) and 25wt% high-density-polyethylene (HDPE). While the binder system of the 3D extrusion was composed of 2wt% of polyvinyl alcohol (PVA) diluted in water. The composition of feedstocks produced are shown in Table 1.

Table 1. Feedstocks composition.

Feedstock label	Amount of graphene (wt. %)	Powder load (wt.%)	Binder system (wt.%)
MIM_Ti-CP	0	60	70 PW / 25 PE / 5 SA
MIM_Ti-0.2GNP	0.2	60	70 PW / 25 PE / 5 SA
MIM_Ti-0.4GNP	0.4	60	70 PW / 25 PE / 5 SA
3D_Ti-CP	0	80	2 PVA / 98 water
3D_Ti-0.3GN	0.3	80	2 PVA / 98 water
3D_Ti-0.5GNP	0.5	80	2 PVA / 98 water

2.2 Experimental Procedure

The preparation process of Ti-xGr samples from MIM feedstocks can be divided in five steps. Firstly, the titanium and graphene powders in the predetermined amount were added into a jar and mixed in roller mixer for 5 hours . In the second step, the titanium/graphene powders were mixed to binder system. For that, PW, PE and SA were added to aluminum cup and heated up to of 150 °C allowing the binders to melt. Then the powders were added under mechanical stirring, the mixture was stirred until completely homogenization. Afterwards the feedstock was cooled to room temperature to solidify. In the third step, MIM feedstocks were molded by warm compaction using a heatable die. For that, MIM feedstock was place in a 9.5 diameter die and heated up to 180 °C, then a pressure of 300 MPa was applied. The amount of feedstock add to the die was adjusted to obtain green samples with 14-18 mm high. The warm compaction approach aimed to achieve similarities with the MIM process while enables the use a smaller amount of feedstock. Although the process is less sophisticated, the fundamental principle remains similar: the feedstock is heated to a temperature above the melting point and molded/compacted. The fourth step is the chemical debinding. During this step, paraffin an stearic acid removal was carried out through a solvent extraction method using an n-hexane bath at a temperature of 60 °C for

a duration of 24 hours. The fifth step is the thermal debinding and sintering. Thermal debinding and sintering were performed in the same cycle in a vacuum furnace. Samples were heated to 500 °C at a heating rate of 2 °C/min and kept at this temperature for 60 minutes in order to remove the residual binder. Subsequently, the temperature was increased to sintering temperature 1200 °C at a heating rate of 10 °C/min. The samples were maintained at the sintering temperature for 120 minutes.

The preparation process of Ti-xGr samples from 3D extrusion feedstocks can be divided in four steps. The first step is the same reported for the MIM feedstock: the titanium and graphene powders are mixed in roller mixer for 5 hours. The second step is the preparation of 3D Extrusion feedstock. First the binder solution was prepared by dissolving 2% PVA in water. Then, the powders were added to the binder solution and stirred until homogeneity paste was achieved. The third step was die compaction of 3D extrusion feedstock. The 3D feedstock was placed into the 9.5 mm diameter die, the amount of feedstock added was adjust to achieve heights ranging from 11 to 14 mm. The feedstock was compacted under 300 MPa was applied for three minutes. The four step is the thermal debinding and sintering, which was performed at same condition reported for the MIM feedstock.

Microstructural characterization was performed in the cross section of polished samples by using scanning electron microscopy (JSM6360, Jeol Technology). Energy Dispersive Spectroscopy (EDS) analysis was performed using a Quantax 75 (Bruker Nano GmbH). The X-ray diffraction analyses were performed on the surface and cross section of Ti-xGNP parts using Brag-Brentano geometry – θ-2θ (Bruker, D8). A Vickers Microhardness was measured in HMV Shimadzu Microhardness tester applying a load of 4.90 N for 15 s following to ASTM E92-82/2003. Elastic modulus was measured by vibroacoustic methods, where samples were tested using a 49 gram load. Porosity was measured by image analysis of SEM images.

3. RESULTS AND DISCUSSIONS

Figure 1 shows SEM image of cross sections of sintered Ti-xGr composites produced from MIM and 3D extrusion feedstocks. The image analysis of SEM images (Table 2) indicated that the graphene addition did not have a significant impact on the sample porosity. On the other hand, feedstock composition has an impact in the porosity: The samples produced from MIM feedstocks (Figures 1(a), 1(b) and 1(c)) exhibit irregular, larger, and less evenly distributed pores compared to samples produced from 3D Extrusion feedstock (1(d), 1(e) and 1(f)). The higher porosity in the samples produced from MIM feedstocks is confirmed by image analysis results shown in Table 2. The higher porosity can be related to the higher amount and the composition of the binder system. MIM feedstocks have a higher amount of binder and are composed of polymers like HDPE, which has higher melting point, that can lead to increased residual porosity during debinding process. Additionally, the SEM image of 3D_Ti-0.5GNP indicated a presence of a second phase. The EDS map of 3D_Ti-0.5GNP (Figure 2) shows that the second phase is rich in carbon, which is an indicative that this phase can be a carbide or a graphene aggregates.

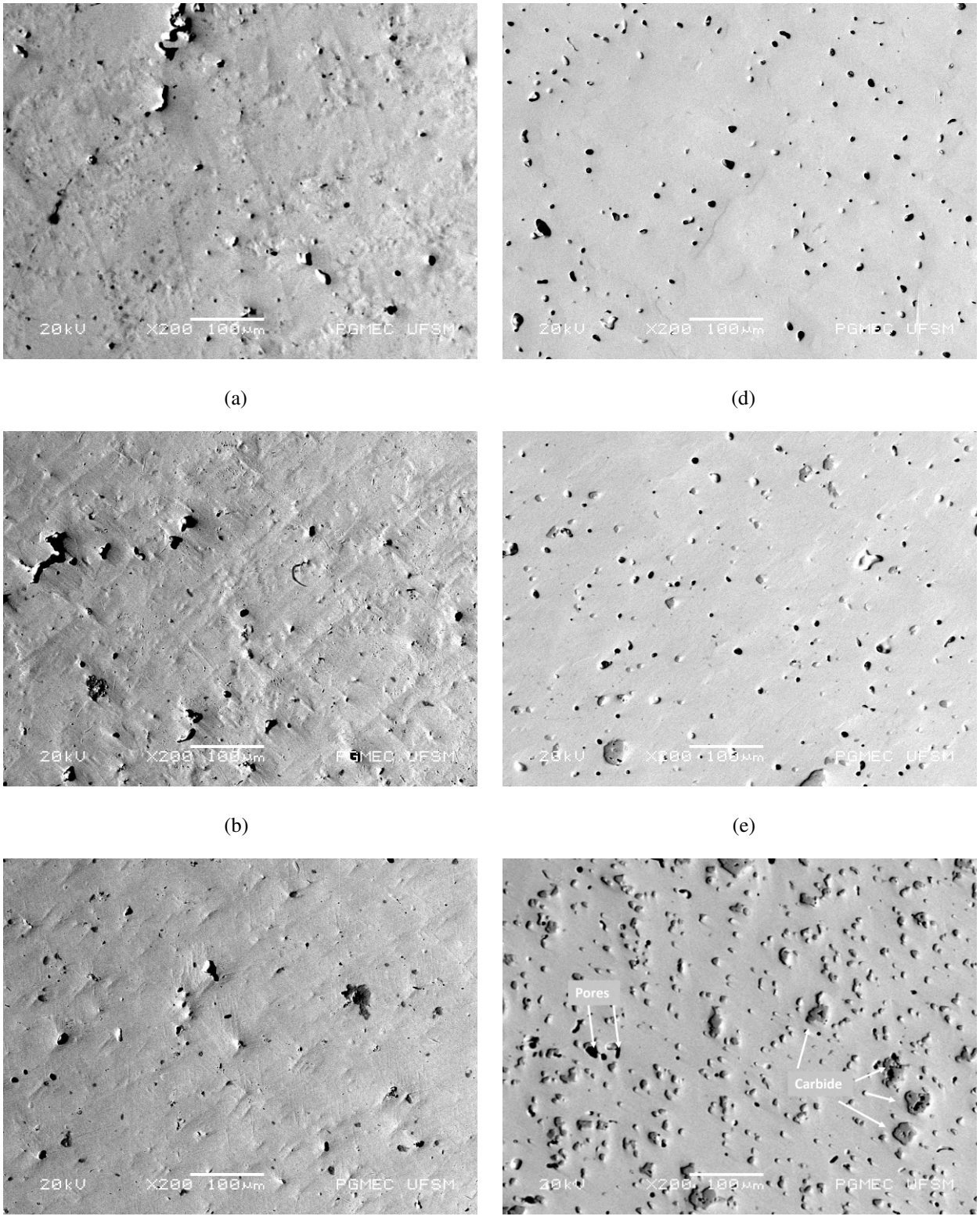

(a) (d)

(b) (e)

(c) (f)

Figure 1. MIM_Ti-CP (a), MIM_Ti-0.2GNP (b), MIM_Ti-0.4GNP (c), 3D_Ti-CP (d), 3D_Ti-0.3GNP (e) 3D_Ti-0.5GNP (f).

The porosity for both group were measured through image analysis using the ImageJ software. Five scanning electron microscopy (SEM) micrographs from different regions of each sample were used for pore counting.

Table 2. Porosity by (SEM) Image.

Sample	**Porosity by Image (%)**
MIM_Ti-CP	3.90 ± 0.59
MIM_Ti-0.2GNP	2.66 ± 0.35
MIM_Ti-0.4GNP	3.05 ± 0.63
3D_Ti-CP	1.87 ± 0.70
3D_Ti-0.3GNP	1.91 ± 0.58
3D_Ti-0.5GNP	2.87 ± 0.47

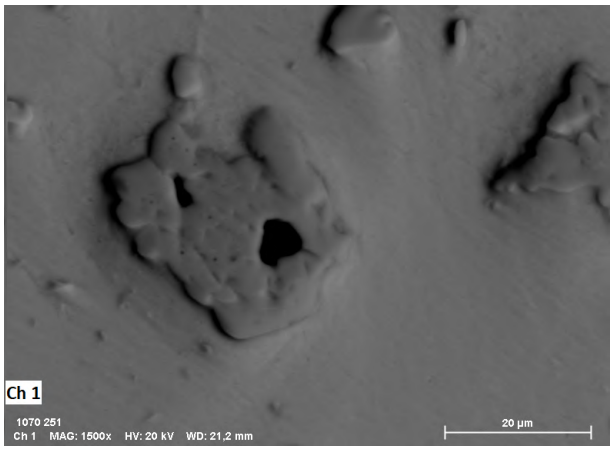

(a)

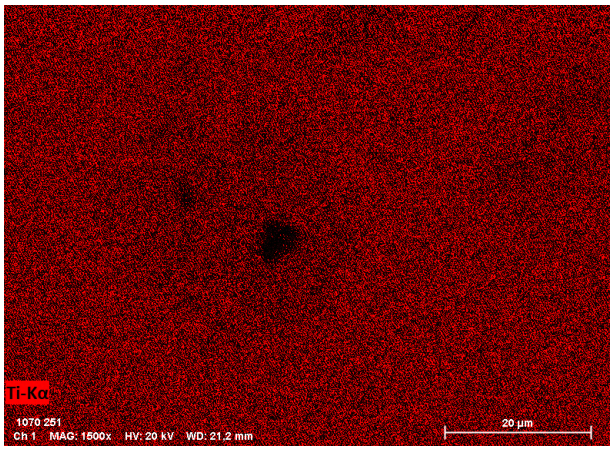

(b)

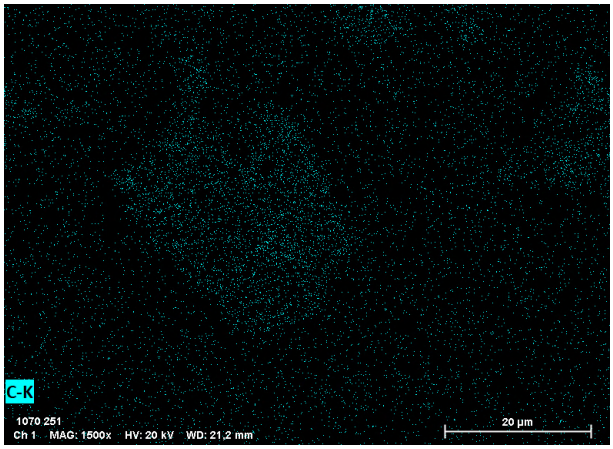

(c)

Figure 2. EDS map of 3D_Ti-0.5GNP. (a) SEM image, (b) Ti map and (c) Carbon map.

The results for the X-ray Diffraction of parts produced from MIM and 3D extrusion feedstocks are shown in Figures 3 and 4, respectively. The peaks in XRD pattern of 3D_Ti-CP and MIM_Ti-CP parts are related to titanium alpha phase, indicating that both Ti_CP parts are composed of Ti alpha phase, which exhibits hexagonal compacted structure. While in the XRD pattern of 3D_Ti-0.3GNP, MIM_Ti-0.4GNP and 3D_Ti-0.5GNP, in addition to the peaks related to the alpha phase, there are peaks in 36, 41, 60, that can be related to a titanium carbide. The presence of peaks related to titanium carbide was only observed in the samples with graphene addition, as well as the results by Cao *et al.* (2017). The intensity of the carbide peaks was higher in 3D_Ti-0.5GNP sample which can be related to the higher amount of graphene in this sample. This result confirms that second phase seen in the SEM image is carbide. XRD and SEM results suggested that graphene diffused to titanium matrix leading to carbide formation.

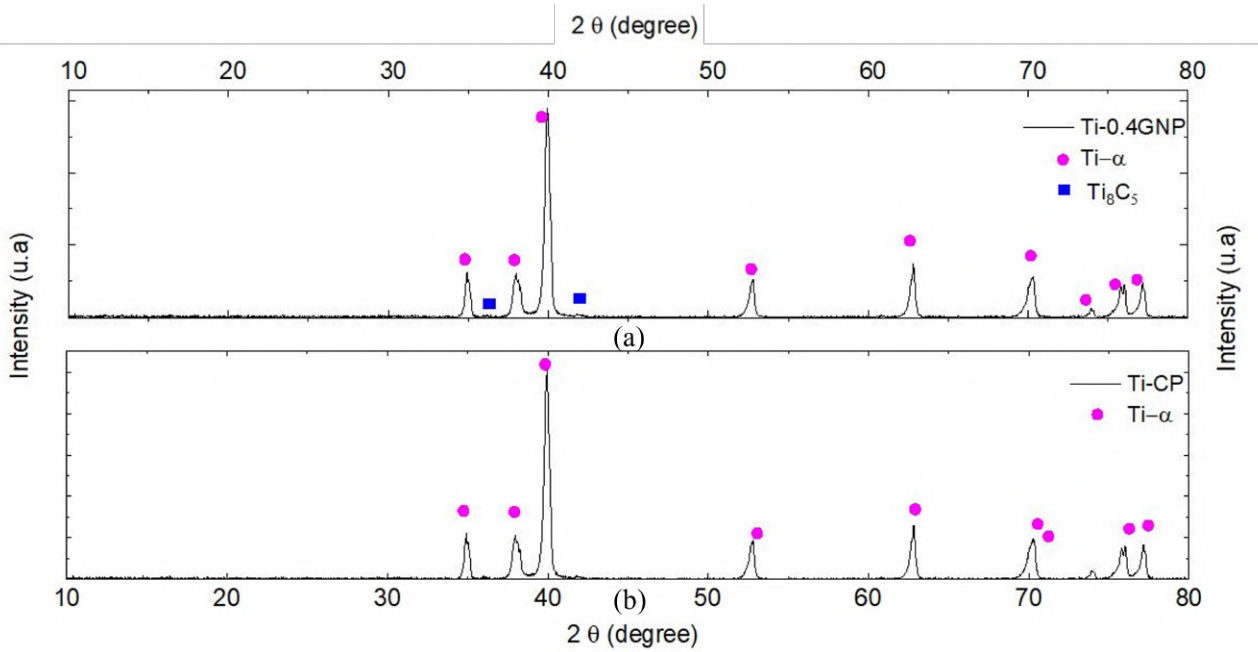

Figure 3. XRD patterns from the cross section of MIM_Ti-0.4GNP (a) and MIM_Ti-CP (b).

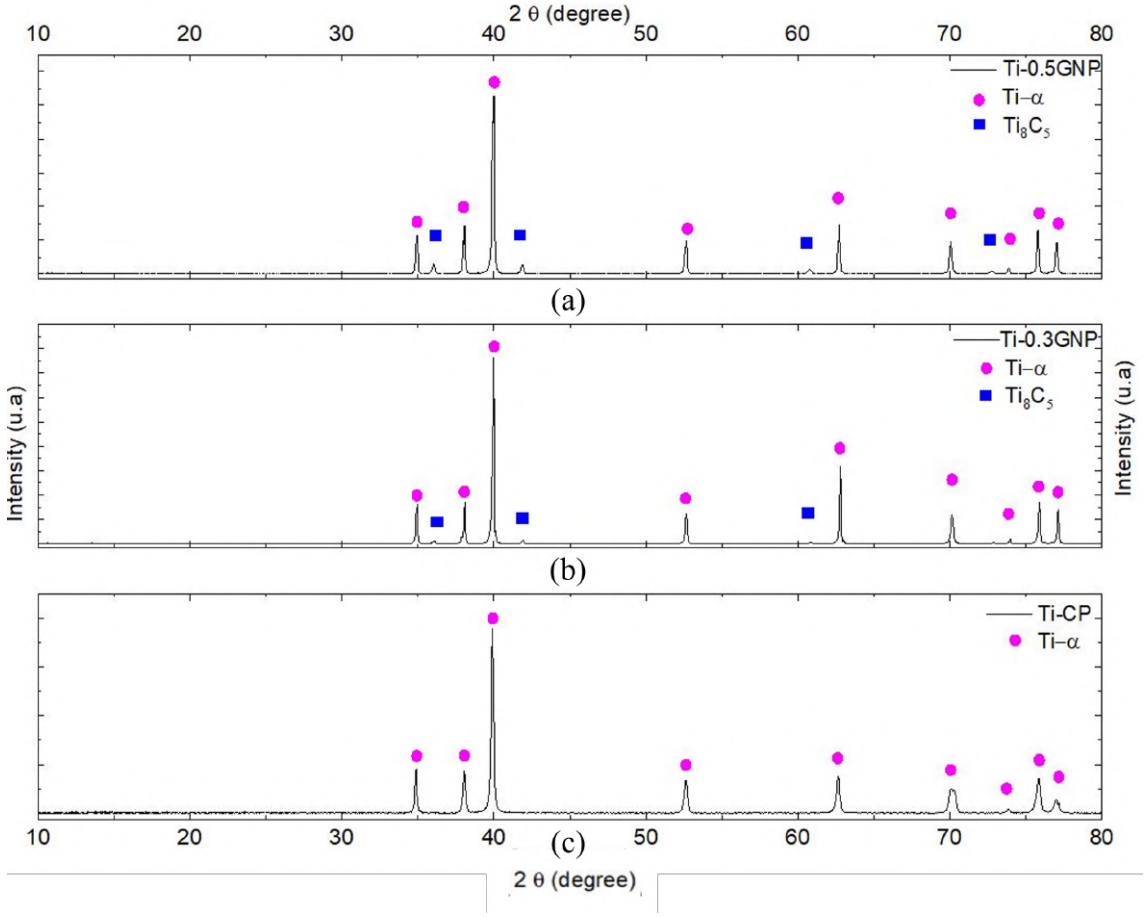

Figure 4. XRD patterns from the cross section of 3D_Ti-0.5GNP (a), 3D_Ti-0.3GNP (b) and 3D_Ti-CP (c).

The results of the hardness test for the samples produced from MIM and 3D extrusion feedstock are shown in Figure 5. The samples produced from MIM feedstock shown a lower hardness which can be associated to their high porosity when compared to samples produced from 3D extrusion feedstocks. In the samples produced from MIM feedstock the graphene addition contributes to a slight reduction of Ti hardness. In the samples produced by MIM feedstock, the high

temperatures and mechanical stirring applied for mixing the powders in the binder system can lead to the deterioration of graphene structure. As consequence the graphene addition of graphene has not a significant effect in the microhardness. In the samples produced from 3D extrusion feedstock the graphene considerable increased the sample hardness. An increase in hardness with graphene was also observed in the literature by (Hu *et al.*, 2018) and (Zhang *et al.*, 2017), – both related the increase of hardness to the formation of small particles of Ti carbides.

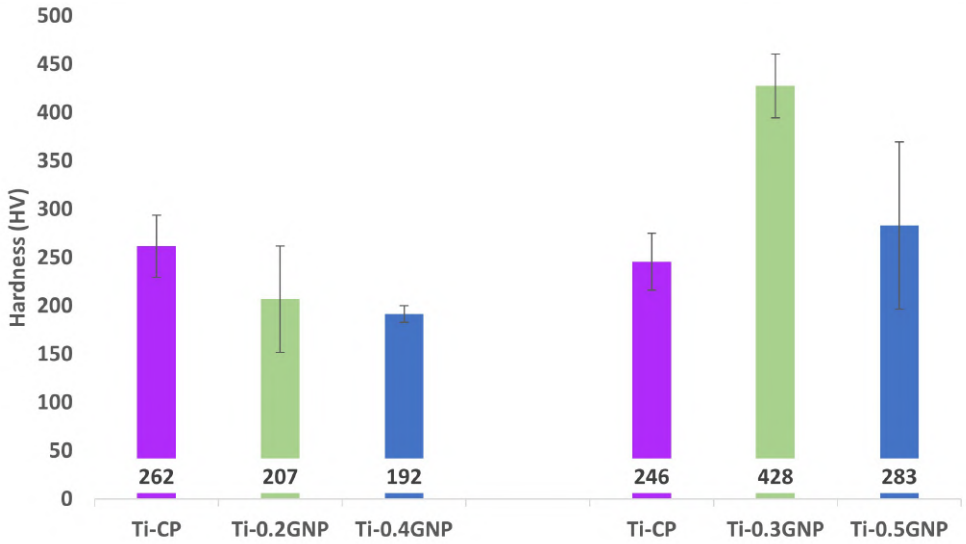

Figure 5. Vickers Microhardness for MIM and 3D feedstocks.

The highest microhardness values were obtained in the 3D_Ti-0.3GNP sample. However, the result for the 3D_Ti-0.5GNP sample showed a reduction in hardness values compared to the 3D_Ti-03GNP. Lower hardness values in the 3D_Ti_0.5GNP sample may be related to the a possible graphene agglomeration during sample preparation and the higher porosity of 3D_Ti-0.5GNP.

The values dynamic elastic modulus for the samples produced form MIM feedstock are shown in Figure 6.

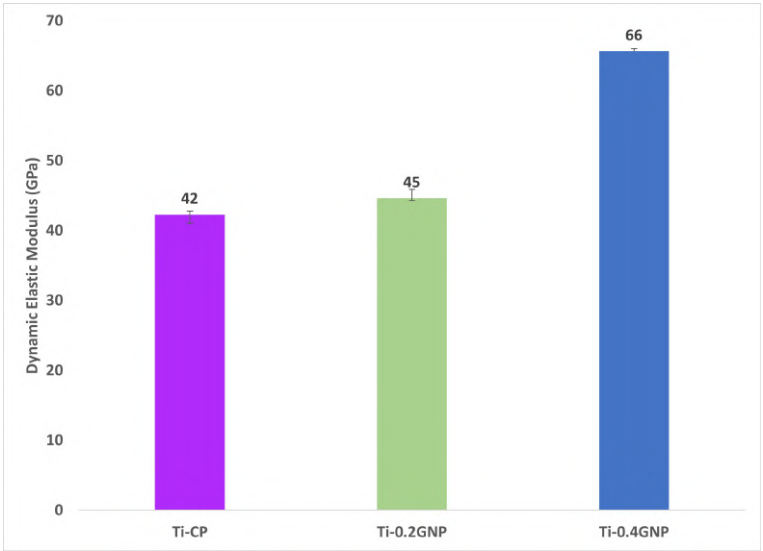

Figure 6. Dynamic Elastic Modulus of MIM.

The addition of graphene increased the elastic modulus of titanium, whereas the samples with 0.4. GNP show a higher elastic modulus than samples produced with 0.2 GNP. The samples produced from 3D Extrusion will be characterized in our ongoing study. Graphene as reported by (Yan *et al.*, 2021) strengths the titanium matrix due to solid solution, grain refinement and manly due the formation of small carbide, which also contribute to improve elastic modulus. The samples showed an increase in the dynamic elastic modulus from 0.2 to 0.4 wt.%GNP. The mass-spring system measures both damping and stiffness of samples. In this case, it is noted that the increase in GNP increased the damping and reduced the vibration of the system.

4. CONCLUSIONS

Graphene reinforced titanium have been successfully fabricated by powder metallurgical routes using compaction of MIM and 3D extrusion feedstocks followed by sintering. The effect of graphene addition, as well as the sample manufacturing process, could be evaluated in terms of microstructure, porosity and mechanical properties. In the samples produced from MIM feedstock, graphene addition has no significat effect on hardness. In contrast, in the samples manufactured by cold compaction of 3D extrusion feedstocks, graphene addition improves hardness. By adding 0.3 wt.% of graphene an improvement of more than 17.0 % in hardness was achieved. The results obtained so far indicated that graphene can be efficiently used as reinforcement for titanium alloys. However, the manufacturing route plays an important role to ensure graphene efficiency as reinforcement material. Therefore, by selecting the suitable manufacturing processes and graphene amount, metal alloys reinforced with graphene have potential for being used as lightweight construction material.

5. REFERENCES

Baril, E., Lefebvre, L.P., Thomas, Y. and Ilinca, F., 2008. "Foam-coated MIM gives new edge to titanium implants". *Metal Powder Report*, Vol. 63, No. 8, pp. 46–55. ISSN 0026-0657. DOI 10.1016/S0026-0657(08)70125-5.

Cao, Z., Wang, X., Li, J., Wu, Y., Zhang, H., Guo, J. and Wang, S., 2017. "Reinforcement with graphene nanoflakes in titanium matrix composites". *Journal of Alloys and Compounds*, Vol. 696, pp. 498–502.

Dehghan-Manshadi, A., Bermingham, M.J., Dargusch, M.S., StJohn, D.H. and Qian, M., 2017. "Metal injection moulding of titanium and titanium alloys: Challenges and recent development". *Powder Technology*, Vol. 319, pp. 289–301. ISSN 1873328X. DOI 10.1016/j.powtec.2017.06.053.

Gialanella, S. and Malandruccolo, A., 2020. *Topics in Mining, Metallurgy and Materials Engineering: Aerospace Alloys*. Springer Nature Switzerland AG, Cham. ISBN 9783030244392.

Gorbatikh, L., Wardle, B.L. and Lomov, S.V., 2016. "Hierarchical lightweight composite materials for structural applications". *Mrs Bulletin*, Vol. 41, No. 9, pp. 672–677.

Hayat, M.D., Jadhav, P.P., Zhang, H., Ray, S. and Cao, P., 2018. "Improving titanium injection moulding feedstock based on PEG/PPC based binder system". *Powder Technology*, Vol. 330, pp. 304–309. ISSN 0032-5910. DOI 10.1016/J.POWTEC.2018.02.043.

Hu, Z., Chen, F., Xu, J., Ma, Z., Guo, H., Chen, C., Nian, Q., Wang, X. and Zhang, M., 2018. "Fabricating graphene-titanium composites by laser sintering pva bonding graphene titanium coating: Microstructure and mechanical properties". *Composites Part B: Engineering*, Vol. 134, pp. 133–140.

Nurhudan, A.I., Supriadi, S., Whulanza, Y. and Saragih, A.S., 2021. "Additive manufacturing of metallic based on extrusion process: A review". *Journal of Manufacturing Processes*, Vol. 66, No. 9, pp. 228–237.

Rane, K. and Strano, M., 2019. "A comprehensive review of extrusion-based additive manufacturing processes for rapid production of metallic and ceramic parts". *Springer Nature*, Vol. 7, No. 8, pp. 155–173.

Saxena, A., Saxena, K.K., Jain, V.K., Rajput, S. and Pathak, B., 2023. "A review of reinforcements and process parameters for powder metallurgy-processed metal matrix composites". *Materials Today: Proceedings*.

Szunerits, S., Peteu, S. and Boukherroub, R., 2015. "Peroxynitrite-sensitive electrochemically active matrices". In S. Szunerits and M. Bayachou, eds., *Peroxynitrite Detection in Biological Media: Challenges and Advances*, Royal Society of Chemistry, pp. 63–77. ISBN 978-1-78262-235-2.

Yan, Q., Chen, B. and Li, J., 2021. "Super-high-strength graphene/titanium composites fabricated by selective laser melting". *Carbon*, Vol. 174, pp. 451–462.

Zhang, X., Song, F., Wei, Z., Yang, W. and Dai, Z., 2017. "Microstructural and mechanical characterization of in-situ tic/ti titanium matrix composites fabricated by graphene/ti sintering reaction". *Materials Science and Engineering: A*, Vol. 705, pp. 153–159.

6. RESPONSIBILITY NOTICE

The authors are solely responsible for the printed material included in this paper.